Power Quality Impacts of an Electric Arc Furnace and Its Compensation

Ahmad Esfandiari*, Mostafa Parniani* and Hossein Mokhtari*

Abstract - This paper presents a new compensating system, which consists of a shunt active filter and passive components for mitigating voltage and current disturbances arising from an Electric Arc Furnace (EAF). A novel control strategy is presented for the shunt active filter. An extended method based on instantaneous power theory in a rotating reference frame is developed for extraction of compensating signals. Since voltages at the point of common coupling contain low frequency interharmonics, conventional methods cannot be used for dc voltage regulation. Therefore, a new method is introduced for this purpose. The passive components limit the fast variations of load currents and mitigate voltage notching at the Point of Common Coupling (PCC). A three-phase electric arc furnace model is used to show power quality improvement through reactive power and harmonic compensation by a shunt active filter using the proposed control method. The system performance is investigated by simulation, which shows improvement in power quality indices such as flicker severity index.

Keywords: electric arc furnace, flicker severity, power quality, shunt active filter, voltage flicker

1. Introduction

Application of nonlinear loads such as adjustable speed drives, electric arc furnaces and power conversion devices in power systems results in power quality problems such as harmonics, interharmonics and voltage fluctuations that force the utilities and consumers to take countermeasure actions. Due to the variety of nonlinear loads and their problems, different compensation systems have been used. Passive filters are conventional solutions to mitigate harmonics. The limitation of passive filters for compensating complex problems such as noninteger harmonics and flicker has made active filters attractive.

Control strategy is the heart of an active filter which substantially affects compensation characteristics. Signal conditioning, compensating signals extraction and command signals generation for the inverter switches are important stages of the control strategy. Frequency and time domain methods can be used for the detection of compensating signals. Selection of the method depends on load characteristics and compensation objectives.

Shunt active filters using traditional control methods have successfully been used to compensate for basic power quality problems such as current harmonics, reactive power and load imbalance [1],[2]. Some loads such as electric arc furnaces draw erratic varying currents which result in severe power quality problems. Reactive power of electric arc furnaces has highly varying feature that requires a fast detection method. Interharmonic components and nonstationary characteristic of current signals make frequency-domain methods in the detection of reference signals inefficient. The reason is that these methods are based on signal transformation and extraction of harmonic components. Another disadvantage of frequency-domain methods is the transfer of energy of signal to side-lobes due to windowing. In time-domain methods, which are based on signal filtering and manipulation, compensating signals have averaged or instantaneous forms.

Electric arc furnace compensation is usually performed by using passive filters, series inductor [3], Static Var Compensators (SVCs) [4]-[7], and Distribution STATic COMpensators (DSTATCOMs) [8]. Passive filters cannot be used for compensating problems such as variable frequency harmonics and flicker. Series inductors may cause reduction of short circuit power and decrease productivity [3]. Although SVCs are effective in mitigating flicker and VAR control, but their performance is limited due to their inherent delays [9]. Moreover, they inject large amount of current harmonics, which need to be filtered. DSTATCOMs compensate only for reactive power at the fundamental frequency.

The instantaneous reactive power theory based on rotating reference frame is presented in [10]-[14] for three-phase four-wire systems for reactive power compensation and neutral current elimination. In this paper, an extended method is used for extracting the compensating signals to suppress the harmonics and to correct the power factor. Also, a new dc voltage control loop is presented that can be used in the presence of noninteger hormonics and flickery voltages at the point of active filter connection. The proposed active filter can improve power quality of highly

* Dept. of Electrical Engineering, Sharif University of Technology, Iran (shesf2000@yahoo.com, parniani@sharif.edu, mokhtari@sharif.edu)
Received June 17, 2005 ; Accepted February 17, 2006

varying loads in three-phase three-wire power systems with unbalanced voltages.

2. System Configuration

Fig. 1 shows the proposed compensating system. It consists of shunt active filter and passive components. The shunt active filter compensates for the load current disturbances and regulates the dc link voltage. The series inductor and shunt capacitor form a passive compensating device. These components limit fast variations of load currents and mitigate voltage notching at the PCC.

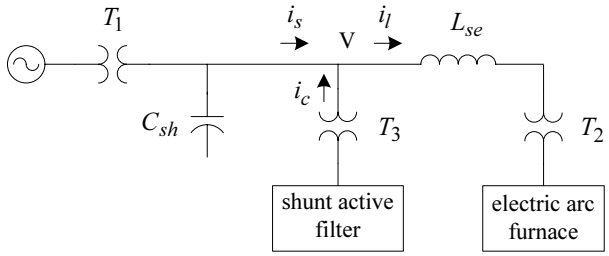

Fig. 1 Basic scheme of a system with an active filter

3. Control Strategy

Instantaneous voltages and currents on the abc coordinates can be transformed into the quadrature $\alpha\beta o$ coordinates. Next, as shown in Fig. 2, $\alpha' qo$ coordinates set is formed by rotating $\alpha\beta$ plane by θ_1 about o-axis so that α-axis aligns with the projection of instantaneous voltage space vector on $\alpha\beta$ plane. Therefore, the

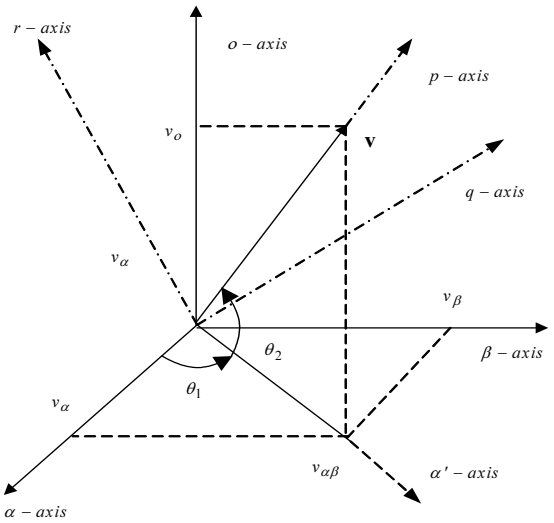

Fig. 2 Relation between $\alpha\beta o$ and pqr reference frames

instantaneous current vector on the $\alpha' qo$ coordinates is obtained by applying the rotating transformation. Then, pqr coordinates is obtained by rotating $\alpha' o$ plane by θ_2 about q-axis so that α'-axis aligns with the projection of instantaneous voltage space vector on $\alpha' o$ plane. The instantaneous current vector on the pqr coordinates can be obtained by applying the rotating transformation. The overall transformation matrix, T, from abc to pqr coordinates is obtained by multiplying the above three transformation matrices. More details can be found in [11],[15].

3.1 Compensating Signal Detection

As shown in Fig. 1, at the PCC, in the abc frame one can write:

$$\begin{bmatrix} i_{sa} \\ i_{sb} \\ i_{sc} \end{bmatrix} + \begin{bmatrix} i_{ca} \\ i_{cb} \\ i_{cc} \end{bmatrix} = \begin{bmatrix} i_{la} \\ i_{lb} \\ i_{lc} \end{bmatrix} \tag{1}$$

Multiplying (1) by the transformation matrix T [15], new current signals in the pqr coordinates are:

$$\begin{bmatrix} i_{sp} \\ i_{sq} \\ i_{sr} \end{bmatrix} + \begin{bmatrix} i_{cp} \\ i_{cq} \\ i_{cr} \end{bmatrix} = \begin{bmatrix} i_{lp} \\ i_{lq} \\ i_{lr} \end{bmatrix} \tag{2}$$

Since the voltage vector is aligned with p-axis, the fundamental frequency component of phase voltages in the pqr frame is a DC value on the p-axis. Other components superimposed on v_p are seen as fluctuating values.

Instantaneous active current of the load current, i. e. i_{lp}, includes a DC value and an oscillatory component. The latter component is an oscillatory active power which should be compensated to achieve a constant active power, i. e.;

$$i_{lp} = \bar{i}_{lp} + \tilde{i}_{lp} \tag{3}$$

where $\bar{i}_{lp}$ and $\tilde{i}_{lp}$ are the DC and fluctuating components of i_{lp}, respectively.

$\tilde{i}_{lp}$ can be extracted by passing i_{lp} through a low pass filter and subtracting the output from i_{lp} [15].

The cutoff frequency of the filter should be low enough to block all disturbance components. On the other hand, a very low bandwidth slows down the dynamic response of

the device.

The EAF load currents may be expressed as:

$$i_a(t) = i_{ma}(t)[i_{fa} + i_{ha}(t)] \quad (4)$$

$$i_b(t) = i_{mb}(t)[i_{fb} + i_{hb}(t)] \quad (5)$$

$$i_c(t) = i_{mc}(t)[i_{fc} + i_{hc}(t)] \quad (6)$$

where i_{ma}, i_{mb} and i_{mc} are amplitude modulating factors causing flicker and i_f and i_h are fundamental and harmonics of currents, respectively. Due to the low frequency of the flicker term, low pass filtering of EAF currents faces the abovementioned drawback, and deteriorates the active filter performance.

An alternative method to remedy this problem is shown in the upper part of Fig. 3. Here, peak values of positive signals $|i_a|$, $|i_b|$ and $|i_c|$ are detected and used to define the amplitude of reference currents. This value is given as:

$$k_i = (i_{am} + i_{bm} + i_{cm})/3 \quad (7)$$

where $i_{im} = \max(|i_i|)$, for i=a,b and c.

Three current templates are obtained by multiplying k_i and the outputs of a sine-wave generator. Then, the resultant vector i_t is tranformed to the *pqr* rotating frame. Thus, i_{tp} would be equivalent to $\bar{i}_{lp}$, and subtracting it from i_{lp} results in load active current disturbance.

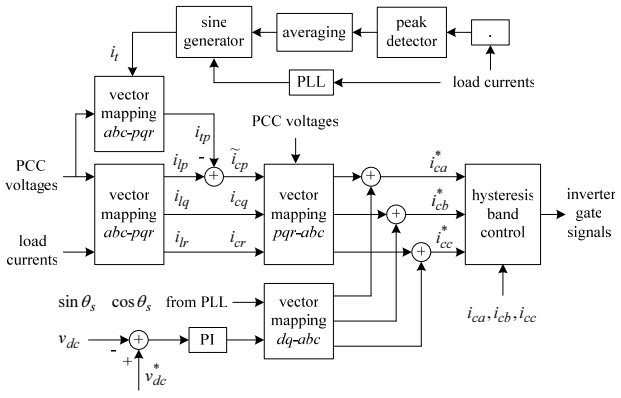

Fig. 3 Controller block diagram

Similarly, instantaneous reactive current i_{lq} has two components. Compensating for the DC component of the reactive power yields power factor correction, whereas compensating its oscillatory component together with the oscillatory active current leads to harmonic elimination and load balancing. Therefore, an ideal compensation requires reference current space vector in *pqr* coordinates be chosen as follows:

$$i^*_{cp} = \tilde{i}_{lp} \quad (8)$$

$$i^*_{cq} = i_{lq} \quad (9)$$

$$i^*_{cr} = i_{lr} = 0 \quad (10)$$

Finally, compensating signals in *abc* frame are obtained as:

$$\begin{bmatrix} i^*_{ca} \\ i^*_{cb} \\ i^*_{cc} \end{bmatrix} = T^{-1} \begin{bmatrix} i^*_{cp} \\ i^*_{cq} \\ i^*_{cr} \end{bmatrix} \quad (11)$$

A hysteresis current controller determines the switching pattern of the inverter devices to achieve the required compensating current. A control block diagram of the shunt active filter is shown in Fig. 3.

3.2 DC Bus Voltage Control

Output voltage of the active filter is generated such that reactive power of the source is reduced. This causes a flow of instantaneous power into the inverter which charges/discharges the inverter dc bus capacitor. Despite the resultant dc bus voltage fluctuations, its average value remains constant in a lossless active filter. However, the converter losses and active power exchange causes this voltage to vary. Regulation of this voltage, which is essential for proper operation of the active filter, requires balancing active power exchange at the fundamental frequency. The inverter is controlled to generate a fundamental frequency current signal in phase with the fundamental frequency voltage at the active filter terminals to regulate the dc bus voltage.

When the active filter terminal voltages and load currents are polluted with noninteger low frequency harmonics, the current vector component which is in-phase with the voltage vector in the rotating reference frame can not be directly used to establish dc voltage control loop. That is because active power exchange occurs at a frequency range including noninteger low frequency terms, and low pass filtering can not be used as explained in [16]. In order to overcome this problem, the difference of measured dc voltage (v_{dc}) and its reference value (v^*_{dc}) is fed to a PI controller. The output of the PI controller is

considered as *d*-axis compensating current component in the synchronous reference frame *dqo*. This signal is transformed to phase currents. Then, the output is used to modify compensating signals. The developed control method is shown in Fig. 3.

4. Electric Arc Furnace Model

In order to simulate the proposed method, a three-phase electric arc furnace model is employed which is composed of two main parts. The first part is based on a dynamic, multi-valued *v-i* characteristic of an electric arc which is obtained by using a general dynamic arc model in the form of a differential equation. The second part of the model consists of Chua's chaotic circuit which represents the arc voltage fluctuations. Detailed information about the model parameters can be found in [17],[18]. This model which is developed in a single-phase form in [17], is extended to a three phase model, and used for the simulations.

5. The IEC Flickermeter

A flickermeter [19], [20] was simulated to evaluate the flicker mitigation of the compensating system. The flickermeter is shown by the block diagram of Fig. 4. The first block dynamically scales the mains rms voltage down to an internal reference level on the basis of a one-minute average. Then block 2 recovers the voltage fluctuations by squaring the scaled input voltage to simulate a lamp behavior. The third block eliminates the DC component and double mains frequency component of the squaring demodulator output. This block is composed of a first order high-pass filter and a sixth order Butterworth low-pass filter. As suggested in [19], the high pass filter has a 0.05 Hz cut-off frequency and the low pass filter has a 35 Hz cut-off frequency. The fourth block weights voltage fluctuations according to the lamp-eye-brain sensitivity. The weighting filter transfer function is specified in Appendix A. Block 5 squares the weighted flicker signal to simulate the nonlinear eye-brain perception. Then, block 6 takes a sliding mean of the signal to simulate the storage effect in the brain. This function is implemented by a first order low-pass filter with a time constant equal to 300 ms, i. e., a cut-off frequency of 0.53 Hz. The output of block 6 represents Instantaneous Flicker Level (IFL). In the following section, IFL will be used to evaluate how the performance of the compensation system. The statistical analysis block consists of a classifier that uses 64 classes. The block analyzes the IFL, using time-at-level statistics over a fixed time interval of 10 min to yield the short-term Flicker Severity index, P_{st} [19],[21]. The index formula is given in Appendix B.

6. Simulation Results

The system in Fig. 1 was simulated using Matlab/ Simulink with the parameters listed in Tables 1 and 2. The PI controller parameters are chosen as $k_p = 0.322$ and $k_i = 0.054$.

Table 1 Parameters of the simulated system

Parameter	Value
Short circuit power, MVA	3500
Shunt active filter inductance, mH	0.045
Shunt active filter resistance, Ohm	0.01
Series inductance, mH	10
DC bus capacitance, mF	14
DC bus voltage, kV	12
Shunt capacitance, μ F	420

Table 2 Parameters of the transformers

Transformer	T_1	T_2	T_3
V_1(kV)/V_2(kV)	220/21	21/0.8	0.7/21
MVA	95	60	20
Resistance, pu	0.005	0.005	0.005
Inductance, pu	0.125	0.1	0.002

6.1 Power Quality Problems

In addition to voltage and current harmonic pollution, an EAF generates other power quality problems such as imbalance, voltage flicker and voltage notching which is

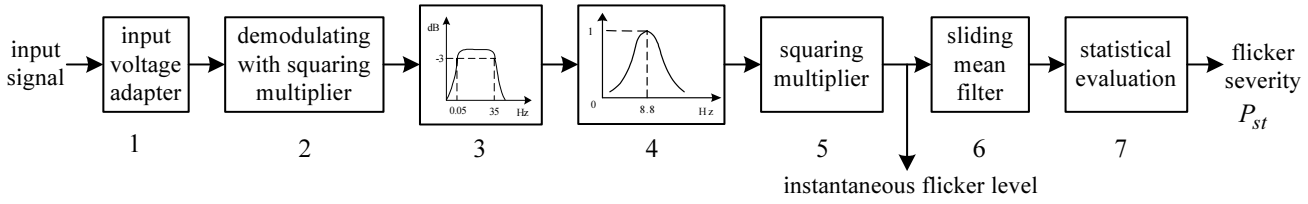

Fig. 4 Block diagram of the IEC flickermeter

caused by arc phenomenon. The latter effect is a high frequency disturbance and makes designing of dc voltage control loop complicated. Figs. 5 and 6 show the voltage disturbances.

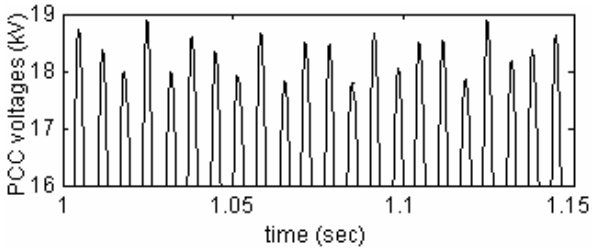

Fig. 5 Three-phase PCC voltages after passive compensation

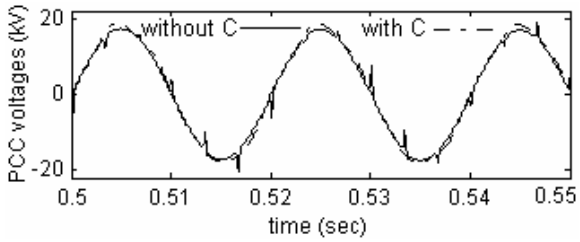

Fig. 6 Shunt capacitor impact on PCC voltage, phase-*a*

Similar problems are observed in the load currents that are depicted in Figs. 7 and 8. Fast Fourier Transform (FFT) of the load current has a continuous distribution of harmonic content. Amplitudes of some of the noticeable harmonic components are mentioned in Table 3.

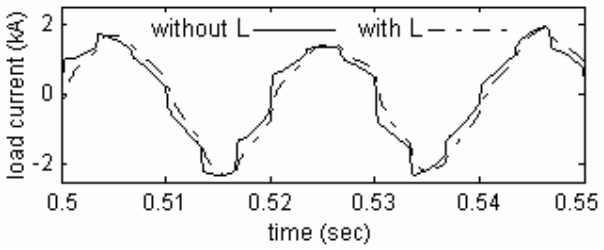

Fig. 7 Series inductor effect on load current, phase-*a*

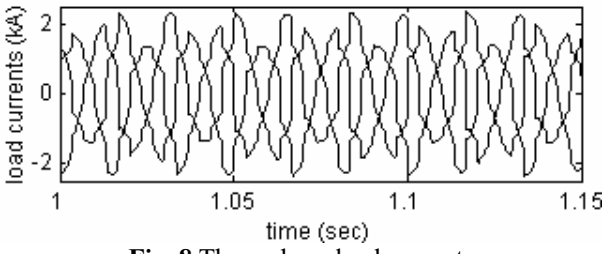

Fig. 8 Three phase load currents

6.2 Compensation Results

At first, voltage notching is compensated by a series inductor and a shunt capacitor as indicated in Fig. 6. Insersion of a series inductor solely, may cause reduction of short circuit power at the point of common coupling which in turn decreases productivity. Whereas the series inductor together with an active filter can be used to mitigate flicker and to improve power factor. Moreover, it is used to limit the highly varying EAF currents and improving active filter performance as shown in Fig. 7.

Figs. 8 and 9 show three phase load and source currents, respectively. FFT of the source current signal befor and after compensation is presented in Table 3. Comparison of harmonic content in load and source currents indicate that in addition to integer harmonics, noninteger harmonics are considerably suppressed.

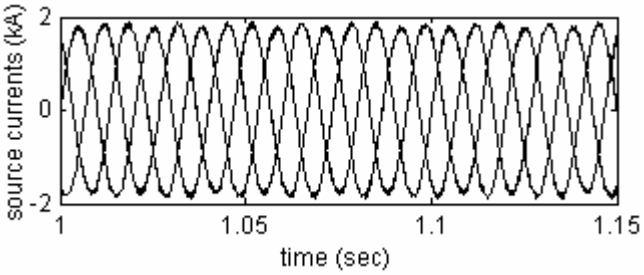

Fig. 9 Source currents

The active filter current contains the varying part of the load current as depicted in Fig. 10. Load and source instantaneous reactive powers are shown in Figs. 11 and 12, respectively. It is observed that the system is capable of compensating for highly varying reactive power.

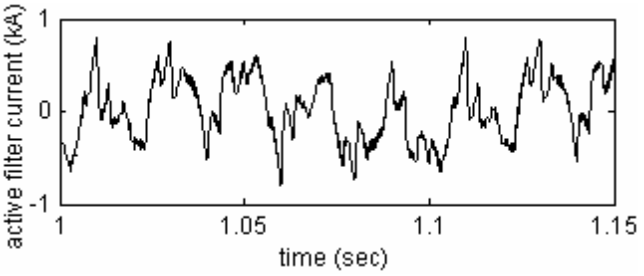

Fig. 10 Shunt active filter current, phase-*a*

The three-phase PCC voltages in Fig. 13 verify reduction of the voltage flicker and imbalance. Frequency

Table 3 Harmonic content of source current

H	10	110	190	250	290	310	350	410	490	550	650	850	950
A1	14.2	9.8	1.4	7.4	1.4	2	4.2	3.2	1.8	1.9	1.5	1	0.9
A2	2.2	1.5	0.0	0.6	0.0	0.0	0.8	0.0	0.0	0.1	0.4	0.12	0.15
H: Harmonic, A1:Harmonic amplitude before compensation, A2: Harmonic amplitude after compensation													

spectrum analysis of the PCC voltage before and after compensation shows the value of 10 Hz component (a non-integer harmonic) befor and after compensation is %0.14 and %0.06, respectively.

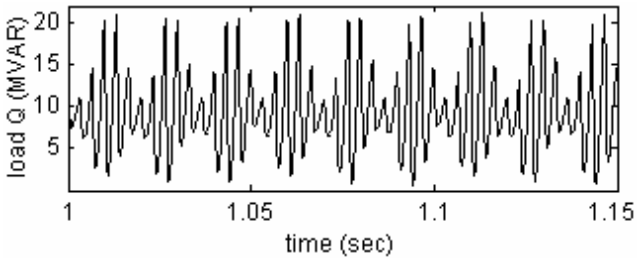

Fig. 11 Load instantaneous reactive power

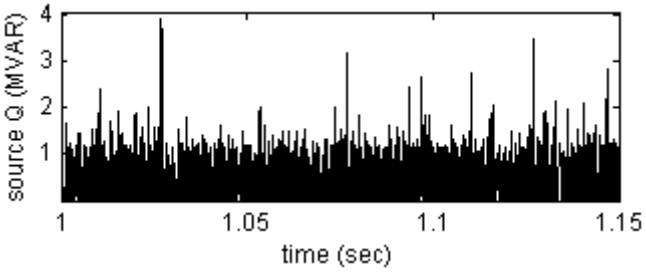

Fig. 12 Source instantaneous reactive power

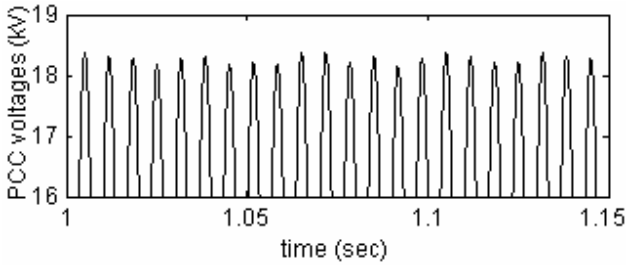

Fig. 13 Three phase PCC voltages after compensation

IFL of the voltage signal before and after compensation is depicted in Fig. 14. The short-term flicker severity index , P_{st} is calculated as described in section 5. This index is changed from 1.3407 to 0.7835 due to the compensator operation. Maximum permissible value of P_{st} level is 1 [19].

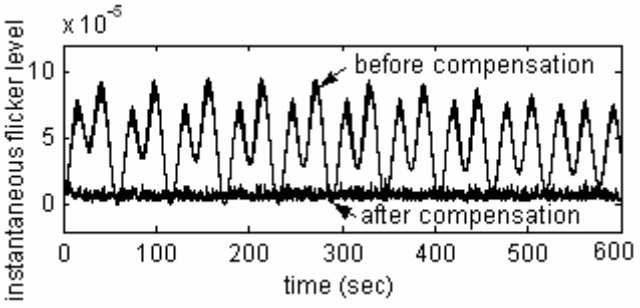

Fig. 14 The IFL of the voltage signal

The other part of the control strategy is the dc voltage regulation. Based on the capacitor voltage shown in Fig. 15, one can see that the proposed voltage control loop offers efficient performance under unbalanced and flickery PCC voltages.

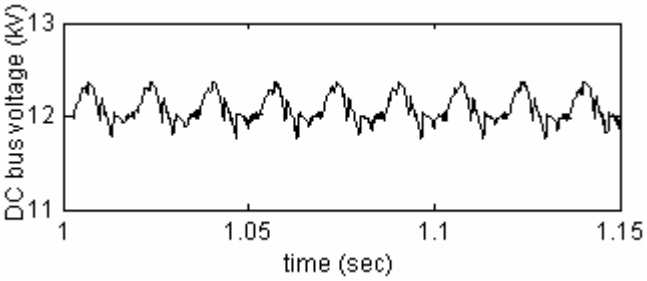

Fig. 15 DC bus capacitor voltage

7. Conclusion

In this paper, a combination of a shunt active filter and passive components is proposed for improving power quality of a system supplying an EAF. The compensator mitigates PCC voltage and load current disturbances, and compensates for reactive power, harmonics, interharmonics, and imbalance. In the proposed scheme, current compensating signals are detected based on generating phase current templates and mapping the current vector onto a rotating reference frame formed by the instantaneous voltages. Alos, since voltages at the point of common coupling contain low frequency interharmonics, conventional methods will not be efficient for dc voltage regulation. Therefore, a new method is introduced for this purpose. Simulation results on a three-phase EAF system model are presented to verify the control strategy and to assess the performance of the compensating system.

8. Apendices

8.1 Appendix A

Transfer function of the weighting filter is given as:

$$F_w(s) = \frac{k\omega_1 s}{s^2 + 2\lambda s + \omega_1^2} \frac{(1 + s/\omega_2)}{(1 + s/\omega_3)(1 + s/\omega_4)} \qquad (12)$$

with

$$k = 1.74802,\ \lambda = 2\pi 4.05981,\ \ \omega_1 = 2\pi 9.15494,$$
$$\omega_2 = 2\pi 2.27979,\ \omega_3 = 2\pi 1.22535,\ \omega_4 = 2\pi 21.9$$

8.2 Appendix B

According to IEC specifications [19],[21], flicker severity index is caculated from:

$$P_{st} = \left(0.0314P_{0.1} + 0.0525P_{1s} + 0.0657P_{3s} + 0.28P_{10s} + 0.08P_{50s}\right)^{1/2} \quad (13)$$

Here the percentiles $P_{0.1}$, P_{1s}, P_{3s}, P_{10s}, P_{50s} are the flicker levels exceeded for 0.1%, 1%, 3%, 10%, and 50% of the time during the observation period. The suffix "s" in the formula indicates that the "smoothed" values should be used. These values are obtained using the following equations:

$$P_{50s} = \left(P_{30} + P_{50} + P_{80}\right)/3 \quad (14)$$

$$P_{10s} = \left(P_6 + P_8 + P_{10} + P_{13} + P_{17}\right)/5 \quad (15)$$

$$P_{3s} = \left(P_{2.2} + P_3 + P_4\right)/3 \quad (16)$$

$$P_{1s} = \left(P_{0.7} + P_1 + P_{1.5}\right)/3 \quad (17)$$

References

[1] W. Dixon, J.J. Garcia, L. Moran, "Control System for Three-Phase Active Power Filter which Simultaneously Compensates Power Factor and Unbalanced Loads," *IEEE Trans. Ind. electron.,* vol. 42, pp. 636-641, Dec. 1995.

[2] B. Singh, K. Al-Haddad, A. Chandra, "A New Control Approach to Three-Phase Active Filter for Harmonics and Reactive Power Compensation," *IEEE Trans. Power Syst.*, vol. 13, pp. 133-138, Feb. 1998.

[3] G.C. Montanari, M. Loggini, L. Pitti, E. Tironi, and D. Zaninelli, "The Effects of Series Inductors for Flicker Reduction in Electric Power Systems Supplying Arc Furnaces," *in Proc. IEEE IAS Annual Meeting,* pp. 1496-1503, 1993.

[4] L. Gyugyi and A.A. Otto, "Static Shunt Compensation for Voltage Flicker Reduction and Power Factor Correction*," in Proc. American Power Conf.*, pp. 1271-1286, 1976.

[5] I. Hosono, M. Yano, M. Takeda, S. Yuya, and S. Sueda, "Suppression and Measurement of Arc Furnace Flicker with a Large Static Var Compensator," *IEEE Trans. Power App. Syst.*, vol. PAS-98, pp. 2276-2282, Nov./Dec. 1979.

[6] A. Wolf and M. Thamodharan, "Reactive Power Reduction in Three-Phase Electric Arc Furnace," *IEEE Trans. Ind. Electron.*, vol. 47, pp. 729-733, Aug. 2000.

[7] C. Surapong, C.Y. Yu, D. Thukaram, D. Nipon, and K. Damrong, "Minimization of the Effects of Harmonics and Voltage Dip Caused by Electric Arc Furnace," *in Proc. IEEE PES Winter Meeting*, pp. 2568-2576, 2000.

[8] J.R. Clouston and J.H. Gurney, "Field Demonstration of a Distribution Static Compensator Used to Mitigate Voltage Flicker," *in Proc. IEEE PES Winter Meeting*, pp. 1138-1141, 1999.

[9] L. Gyugyi, "Dynamic Compensation of AC Transmission Lines by Solid-State Synchronous Voltage Sources," *IEEE Trans. Power Deliv,* vol. 9, pp. 904-911, Apr. 1994.

[10] H. Kim, H. Akagi, "The Instantaneous Power Theory Based on Mapping Matrices in Three- Phase Four-Wire Systems," *in Proc. Power Conversion Conf.*, pp. 361-366, 1997.

[11] H. Kim, H. Akagi, "The Instantaneous Power Theory on the Rotating p-q-r Reference Frames," *in Proc. IEEE Int. Conf. on Power Electronics and Drive Systems*, pp. 422-427, 1999.

[12] F. Z. Peng, G. W. Ott, D. J. Adams, "Harmonic and Reactive Power Compensation Based on the Generalized Instantaneous Reactive Power Theory for Three-Phase Four-Wire Systems," *IEEE Trans. Power Electron.*, vol. 13, pp. 1174-1181, Nov. 1998.

[13] F. Z. Peng, J. Lai, "Generalized Instantaneous Reactive Power Theory for Three-Phase Power Systems," *IEEE Trans. Instrument. and Meas.*, vol. 45, pp. 293-297, Feb. 1996.

[14] H. Akagi, S. Ogasawara, and H. Kim, "The Theory of Instantaneous Power in There-Phase Four-Wire Systems: A Comprehensive Approach," *in Proc. IEEE IAS Annual Meeting*, pp. 431-439, 1999.

[15] A. Esfandiari, M. Parniani, and H. Mokhtari, "A New Control Strategy of Shunt Active Filters for Power Quality Improvement of Highly and Randomly Varying Loads" *in Proc. Int. Symposium on Industrial Electronic*s, pp. 1297- 1302, 2004.

[16] A. Esfandiari, M. Parniani, H. Mokhtari, "Shunt Active Filter Control based on Instantaneous Power Theory on a Rotating Reference Frame in 3-Phase System," presented at the *11th Int. Power Electronics and Motion Control Conf.*, Riga, Latvia, 2004.

[17] O. Ozgun, A. Abur, "Flicker Study Using a Novel Arc Furnace Model," *IEEE Trans. PowerDeliv.*, vol. 17, pp. 1158-1163, Oct. 2002.

[18] E. O'Neill-Carrillo, G.T. Heydt, E.J. Kostelich, S.S. Venkata, and A. Sundaran, "Nonlinear Deterministic Modeling of Highly Varying Loads," *IEEE Trans. Power Deliv.*, vol. 14, pp. 537-542, Apr. 1999.

[19] International Electrotechnical Commission, IEC 61000-4-15, Testing and measurement techniques—Section 15: Flickermeter—Functional and design specifications, 1997.

[20] A. Hernández, J.G. Mayordomo*,* R. Asensi, and L.F. Beites, "A New Frequency Domain Approach for Flicker Evaluation of Arc Furnaces," *IEEE Trans. Power Deliv.*, vol. 18, pp. 631-638, Apr. 2003.

[21] International Electrotechnical Commission, IEC 868, Flickermeter- Part 0: Evaluation of Flicker Severity, 1991.
[22] T. Keppler, N. Watson, and J. Arrillaga, "Computation of the Short-Term Flicker Severity Index," *IEEE Trans. Power Deliv.*, vol. 15, pp. 1110-1115, Oct. 2000.

Ahmad Esfandiari
He was born in Sarband, Iran in 1973. He received the B.Sc. and M.Sc. degrees in electrical engineering from Sharif University of Technology, Tehran, Iran, in 1996 and 1998, respectively. His interests include applications of power electronics, and power quality.

Mostafa Parniani
He obtained his B.Sc. and M.Sc. degrees in Electrical Power Engineering from Tehran Polytechnic and Sharif University of Technology (SUT), in 1987 and 1990 respectively; and Ph.D. in Electrical Engineering from the University of Toronto in 1995. Since then, he has been with the Electrical Engineering Dept. of SUT as an assistant professor. He is currently a visiting scholar at Rensselaer Polytechnic Institute, USA. In the past, he has worked with Ghods Niroo Consulting Engineers Co., Electric Power Research Center, and Niroo Research Institute. He has also been a member of IEEE Task Force on Slow Transients, as well as several national committees in his field. His areas of interest are power system control and dynamics, reactive power control, and applications of power electronics in power systems.

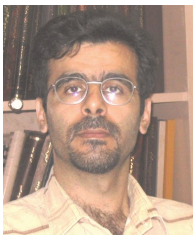

Hossein Mokhtari
He was born in Tehran, Iran. He received this B.Sc. degree in electrical engineering from Tehran University, Tehran, Iran in 1989. He worked as a consultant engineer for Electric Power Research Center (EPRC) in Tehran in dispatching projects. In 1994, He received his M.A.Sc. degree from University of New Brunswick, Fredericton, N.B., Canada. He obtained his Ph.D. degree in electrical engineering from the University of Toronto in 1998. He is currently an associate professor in the Electrical Engineering Department of Sharif University of Technology. His research interests includes power quality and power electronics.